Available online at www.sciencedirect.com
SCIENCE DIRECT®
Vision Research 45 (2005) 1957–1965
Vision Research
www.elsevier.com/locate/visres

Investigating the light absorption in a single pass through the photoreceptor layer by means of the lipofuscin fluorescence

Pedro M. Prieto [a,*], James S. McLellan [b], Stephen A. Burns [b]

[a] Laboratorio de Optica, Universidad de Murcia, Edificio C, Campus de Espinardo, E-30071 Murcia, Spain
[b] Schepens Eye Research Institute, 20 Staniford St., Boston, MA 02114, USA

Received 1 October 2004; received in revised form 19 January 2005

Abstract

Reflection densitometry has been widely used to measure the density difference of the bleachable cone photopigments in human eyes. Most such measurements make a series of assumptions concerning the amount of scattered light to derive an estimate of the true cone photopigment density from the density difference measurements. The current study made three types of measurements of the light returning from the eye before and after bleaching: the amount of light returning in the "directed" reflection, which is a double-pass estimate of the cone photopigment density; the amount of light in undirected or diffuse reflection; and the amount of fluorescence from lipofuscin in the RPE, which provides a single-pass measurement of optical density difference. For a 1 deg foveally fixated field, the density difference estimates for the three measurements were 0.68, 0.21, and 0.22 respectively. The lipofuscin fluorescence was found to be unguided. The background density difference was non-negligible and very close to the single pass estimate from fluorescence. These measurements each involve potentially different pathways of light through the retina, and therefore place different constraints on models of these pathways. A simple model comparing the directional and the fluorescence optical densities produced retinal coverage estimates around 70–75%. Estimates of the shape factor of the single pass optical Stiles–Crawford effect were evaluated from the dark-adapted and bleached fluorescence measurements. The values were closer to those obtained from psychophysical methods than to the double pass optical Stiles–Crawford shape factors obtained directly from retinal reflectometry.

Keywords: Photopigment optical density; Photoreceptor physical property; Lipofuscin fluorescence; Optical Stiles–Crawford effect

1. Introduction

In the first step in the visual process, light collected by the cone photoreceptors is absorbed by photopigments and transduced into neural signals. The major limiting factors in the collection and absorption of light are the total optical density of the photopigment present in one cone and the degree of coverage of the retina by the cone apertures. Both of these parameters are influenced by the wave-guiding properties of the cone photoreceptors, which increase the effective optical density for a fixed amount of photopigment and modify the effective cone apertures due to angular tuning. Retinal reflectometry and densitometry have successfully provided means for probing the combined influence of these parameters and for examining the physical properties of the photoreceptors, by providing in vivo estimates of the total photopigment in the eye (Elsner, Burns, Hughes, & Webb, 1992, 1993; Kilbride, Read, Fishman, & Fishman, 1983; Marcos, Tornow, Elsner, & Navarro, 1997; Rushton, 1958; Tornow, Beuel, & Zrenner, 1997; van Norren & van de Kraats, 1989), and of cone directionality (Burns, Wu, Delori, & Elsner, 1995; DeLint, Berendschot, & van Norren, 1997; Gorrand & Delori,

* Corresponding author. Tel.: +34 968 367281; fax: +34 968 363528.
E-mail address: pegrito@um.es (P.M. Prieto).

0042-6989/$ - see front matter © 2005 Elsevier Ltd. All rights reserved.
doi:10.1016/j.visres.2005.01.023

1995; He, Marcos, & Burns, 1999; Marcos & Burns, 1999; van Blokland, 1986; Vohnsen, Iglesias, & Artal, 2004).

Precise quantification of the optical density of the photopigment in the cones has been difficult, and increasingly detailed models of the interaction of light with the retina have been developed to improve these estimates (for a recent review see Berendschot, DeLint, & van Norren, 2003). In general, densitometry has provided somewhat lower estimates of the optical density of the cones than have psychophysical techniques (Elsner, Burns, & Webb, 1993). To address this apparent discrepancy, van de Kraats, Berendschot, and van Norren (1996), developed a reflection model which incorporates inter-reflection from the discs of the cones. However, one of the main limitations in developing models of reflectometry has been the lack of detailed data on the light paths through which the cone photopigments are sampled in retinal densitometry.

The waveguide properties of the cones affect not only the absorption of light, but also the reflection of unabsorbed light back through the pupil. The amount of light efficiently coupled with the cones depends on the angle of the cone apertures with respect to the pupil. For light incident on the retina, this angular tuning is responsible for the Stiles–Crawford (SC) effect (Stiles & Crawford, 1933). For light returning through the pupil from the retina, this angular tuning produces a Gaussian distribution of light, an effect termed the optical Stiles–Crawford effect (OSC), which is maximal when the pupil position of the incoming light matches the angular tuning of the cones. The OSC has been exploited in retinal densitometry by comparing these distributions under bleached and dark-adapted conditions. However, these pupillary distributions of light represent the combined contribution of number of different light pathways through the photoreceptor layer, some of them directional and some non-directional (van Blokland, 1986). This combination makes it difficult to extract information about individual properties of the photoreceptors, such as retinal coverage proportion, photopigment optical density, path length through the outer segment, etc. In addition, psychophysical measurements and optical measurements of angular tuning are different (He et al., 1999) suggesting that multiple factors beyond cone collection efficiency are involved in the optical measurements (Marcos, Burns, & He, 1998).

The current paper uses the spatial variation in the reflection of light from the retina together with the fluorescence of the retinal lipofuscin (Delori et al., 1995) to better constrain models of densitometry. Lipofuscin is useful for this, because it is located posterior to the photoreceptors in the retinal pigment epithelium (RPE). Lipofuscin was excited with a wavelength that is well absorbed by photopigment, and fluorescence was measured at a longer, minimally-absorbed wavelength. By applying a simple model of light pathways and combining single- and double-pass estimates of photopigment optical density under fully bleached and regenerated conditions, we produced an in vivo estimate of the cone coverage, and by comparing the fluorescence levels obtained with the photopigments bleached and fully regenerated for different pupil positions, we obtained a single pass estimate of the OSC peak width.

2. Methods

2.1. Apparatus

We used a slightly modified version of the imaging reflectometer described previously (Burns et al., 1995). This device was developed to measure the intensity distribution in the pupil plane produced by the retinal reflection of light illuminating the eye in Maxwellian view. It consists of four separate channels: (1) The illumination channel uses a 543 nm laser to project a 4.5-log Troland 1-deg field onto the retina through an 18 μm pinhole conjugate to the subject's pupil. The location of this pinhole in the pupil plane is computer controlled, allowing variation in the direction of the light incident on the cone mosaic. (2) The detection channel contains a cooled, 16-bit CCD camera (Princeton Instruments), which images the light distribution returning from the retina at the pupil plane. An aperture in a retinal conjugate plane limits the measurement to light coming from a 2 deg retinal area surrounding the stimulus. For fluorescence measurements, a filter is placed in front of the camera, with a log density >5 for $\lambda < 560$ nm and ~0 for $\lambda > 560$ nm. (3) The bleaching channel uses a 592 nm laser to produce an 8 deg, 5.7-log Trolands illumination field through a 4-mm entry pupil, sufficient to bleach >95% of the photopigment in the illuminated area. The bleaching light always entered the eye through the center of the pupil. (4) The fixation channel provides a 633 nm test aligned with both the illumination, detection, and bleaching fields. Intensity was less than 3-log Trolands.

Since pupil alignment is critical, a monitoring system was used to frequently check the location of the eye's pupil relative to the instrument pupil. This system consisted of an IR diode illuminating the subject's eye and a mobile mirror in the measurement channel directing light to a video camera focused at the pupil plane. Pupil images where displayed on a monitor with a series of circles concentric with the measurement, bleaching and fixation channels. The operator used these images to focus and center the subject's pupil by moving the head with a three-axis control.

Before each image, the bleaching and fixation channels were blocked and the IR diode of the pupil monitoring system was switched off.

2.2. Procedure

Measurements of the intensity distribution in the pupil plane produced by light from either retinal reflection or fluorescence were collected for both dark-adapted and bleached conditions. Images for different entry pupil positions were recorded for each experimental condition. A typical session consisted of four blocks: dark-adapted reflectometry, dark-adapted fluorescence, bleached reflectometry, and bleached fluorescence. In order to prevent the slow changes in the optical behavior of the cones reported by DeLint, Berendschot, van de Kraats, and van Norren (2000), we started each experimental session with the dark-adapted measurements. The subjects wore an eye patch for 30 min before the first image was taken. Bleaching of the photopigments, required for the last two blocks, was produced by opening the bleaching channel for 1 min before continuing the experiment. To maintain a constant bleach state, the bleaching light was switched off only during the measurement (approximately 10 s off, for each minute).

Control experiments were performed to ascertain that no appreciable bleaching was produced by either the fixation light or the measurement light at the fastest image acquisition rate achievable with our apparatus and control software. The OSC peak for each subject was also determined during these control experiments, by searching for the illumination position that maximized the directional peak of retinal reflection.

Each experimental block consisted of two series of 15 images: 13 images for pupil entry positions configured on a rhombus-shaped grid at 1 mm spacing around the OSC peak of the subject (see Fig. 2); one additional image with on-peak illumination; and one far off-peak image (at least 2 mm vertically and 2 mm horizontally outside the OSC peak). Although the OSC peak was the origin for the scanning, the actual reference point for positioning was the pupil center, which was aligned with the fixation channel, the bleaching channel and the zero-displacement illumination channel. If the pupil moved appreciably, extra images for the illumination positions involved were taken. Additional frames were also recorded when either the subject or the operator noticed any problem, e.g., blinking or incorrect fixation.

Exposure time was 1 s both for reflectometry and fluorescence images. On-chip 5×5 pixel binning was used to reduce the electronic noise. Typical duration of the whole session was around 2 h.

2.3. Subjects

The right eyes of three normal male subjects were studied. Ages were 30 (FV), 33 (PP), and 36 (JM). Although subject JM has deuteranomalous color vision, this was not expected to influence the current experiment and no significant differences were found. The position of each subject's OSC peak was referred to the subject's dilated pupil center, and expressed as a (horizontal, vertical) vector in millimeter, with positive values standing for temporal and superior displacements. Peak positions were $(0,-1)$ for FV, $(1,0)$ for PP, and $(1.5,0)$ for JM. For each subject, three sessions were conducted, typically one month apart. After informed consent was obtained, subjects were dilated with 1% Tropicamide.

2.4. Data processing

Spatially resolved optical density difference (ODD) due to bleaching was calculated for each pixel as the logarithm of the ratio between the intensities for the dark-adapted and bleached eye for the same illumination entry location. However, this estimate would be biased by stray light or by pupil decentering. As a consequence, before the density difference was calculated, it was necessary to process the images to correct for stray light and to recenter the pupil. This processing was performed on both the reflectometry and fluorescence images using a set of tools programmed in MATLAB (Mathworks, Inc., Natick, MA). Two kinds of stray light were detected and compensated for: a background level and a narrow peak. The background level was estimated from a section in the images outside the system pupil (Burns, Wu, He, & Elsner, 1997). The narrow peak was approximately four pixels in width and its location was perfectly correlated to the illumination entry pupil location (as determined in pilot experiments and see Section 3, Figs. 1 and 2), and did not change in intensity with the bleaching state of the retina. It appeared in both the reflectometry and fluorescence images, though arising from a different source in each case. In the reflectometry images, this peak is assumed to have come from scattering in the cornea, since it does not behave as a specular corneal reflection. In the fluorescence images, this scattering is completely removed by the orange filter and, therefore, lens fluorescence is the most likely source of the peak. In both cases, the peak was compensated by substituting the intensity in a region of five pixels around the peak maximum by the mean intensity in a 1-pixel ring around this region.

Pupil recentering was performed by calculating and shifting the center of the circle best fitting the pupil (Burns et al., 1997). This procedure was required to compensate slight pupil movements not detected and corrected during the experiment using the pupil monitor system. By recentering all the images, we assure that the pixel-to-pixel ratio between images is the ratio between intensities exiting through the same pupil point. However, pupil movements also mean a shift in the illumination entry position relative to the OSC peak. This effect cannot be easily corrected in the processing stage. As a consequence, we discarded images where pupil

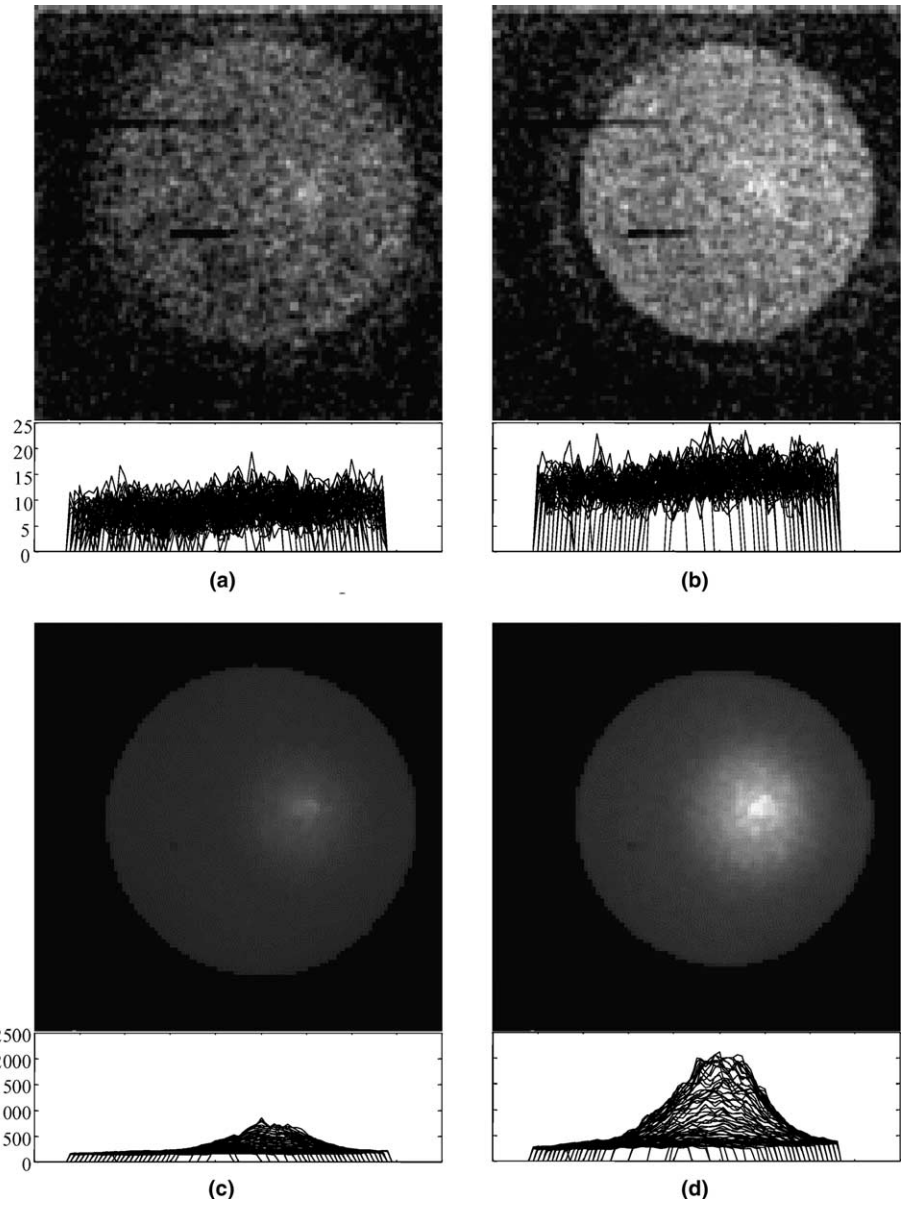

Fig. 1. Example of pupil plane images obtained for each of the blocks comprised in an experimental run: (a) dark-adapted fluorescence, (b) bleached fluorescence, (c) dark-adapted reflectometry, and (d) bleached reflectometry. The images were obtained for on-peak illumination in one of the runs on subject PP. Below each image, the intensity inside the pupil has been plotted to give an idea of both the profile and the intensity levels involved. The scale (in the arbitrary units provided by the camera) was the same for panels (a) and (b) and for panels (c) and (d).

decentering exceeded 0.5 mm in any direction from the mean pupil position through the experiment session.

In the reflectometry images, two different light components were considered: the directional component and the multiply scattered background. The scattered light level was calculated by fitting the reflection intensity to a Gaussian shape plus a background level. By subtracting this background from the image, the spatial distribution of the directional component in the pupil plane was then calculated. Alternatively, another background estimate was obtained by averaging the intensity on a region far from the OSC peak but inside the subject's pupil. Although small differences were occasionally found between the background estimates produced by these two methods, the differences induced in the ODD values were smaller or on the order of the typical standard deviation of the estimates. The results shown in this work are based on the background estimates obtained by Gaussian fitting. Each component of the retinal reflection was used to obtain a different ODD estimate. The background optical density difference (ODD_b) was evaluated from the background levels obtained by fitting. The directional components of the images were used to obtain pixel-to-pixel optical density differences, the maximum value of which is taken as the directional optical density difference (ODD_d).

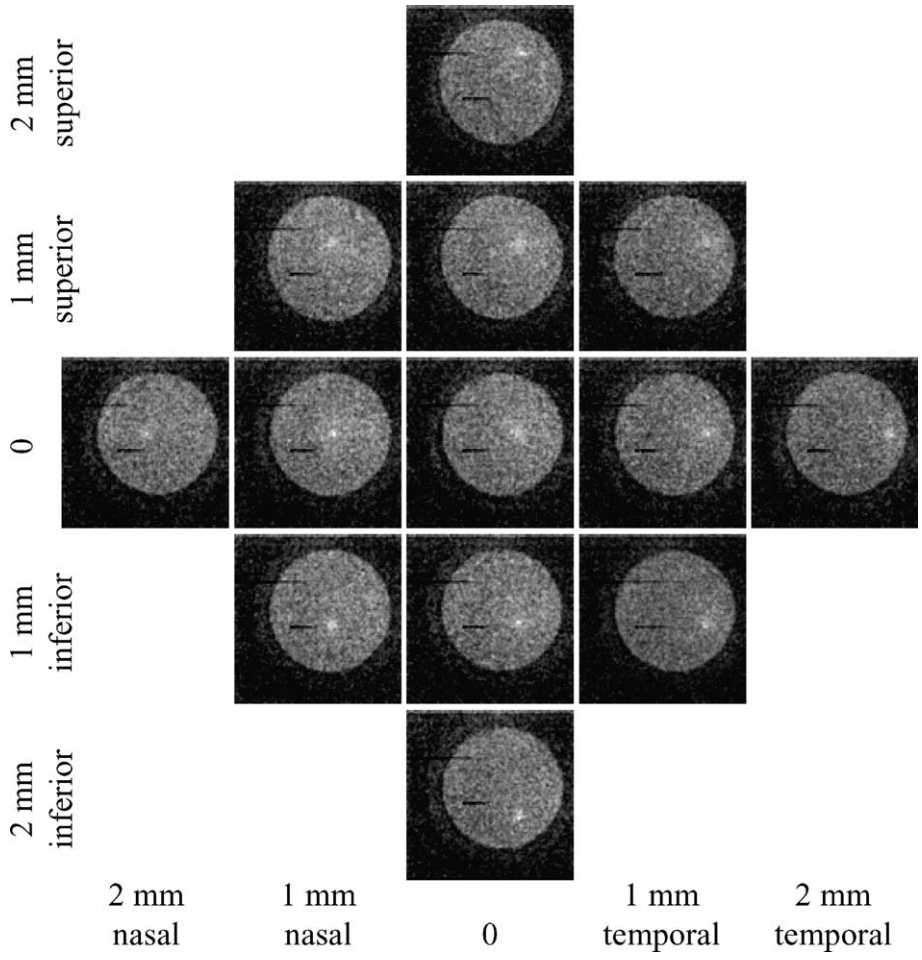

Fig. 2. Set of bleached fluorescence images for subject PP for different entry positions of the illumination beam. The labels stand for the illumination location with respect to the OSC peak. The shallow peak attributed to lens fluorescence (see text) can be seen to closely follow the illumination displacements.

For the fluorescence images, the pixel-to-pixel ODD is very noisy due to the low intensity levels involved. However, since the fluorescence is not directional (see Sections 3 and 4), we obtained estimates of the fluorescence intensity level by averaging pixels inside the subject's pupil. The fluorescence optical density difference (ODD_f) was obtained from these mean values.

3. Results

Within a run, the ODD estimates were evaluated for all the possible combinations of one dark-adapted image and one bleached image for each illumination location and measurement type. Table 1 gives the average values obtained for these pairings for each subject. Fig. 1 shows one image representative of each experimental block for subject PP. The plots below each image correspond to single exposures for on-peak illumination and represent the light level in the pupil plane coming from retinal reflection or fluorescence, with either dark-adapted or bleached photopigment.

Although the intensity level of lipofuscin fluorescence is approximately 2 orders of magnitude lower than the intensities obtained from the retinal reflection, fluorescence measurements produce a measurable intensity distribution in the pupil plane. Furthermore, by comparing panels (a) and (b) in Fig. 1, it can be seen that the fluorescence level is sensitive to photopigment bleaching. As expected, the fluorescence level is higher when the cone photopigments are bleached, since more excitation light reaches the RPE. For our illumination wavelength, lipofuscin generates a broad fluorescence spectrum spread across the red and near IR (Delori, 1994), peaking in the vicinity of 620 nm. Convolution of the fluorescence spectrum with our blocking filter indicates that there is minimal impact of photopigment absorption on the emitted light distribution. Therefore, the change in fluorescence with bleaching must be due to differences in the passage of the excitation (green) light through the photoreceptor layer in the dark-adapted and bleached

Table 1
Parameters calculated from each experimental run together with the mean across runs for each subject and the standard error

Subject	Run	Directional ODD_d	Background ODD_b	Fluorescence ODD_f	Coverage	Shape factor ρ
FV	1	0.719	0.211	0.221	0.708	0.0648
	2	0.776	0.262	0.257	0.756	0.0393
	3	0.678	0.212	0.206	0.697	0.0617
	Mean	**0.724**	**0.229**	**0.228**	**0.721**	**0.0553**
	Standard error	0.028	0.017	0.015	0.018	0.0080
JM	1	0.726	0.213	0.220	0.702	0.0783
	2	0.692	0.167	0.196	0.661	0.0519
	3	0.737	0.265	0.250	0.765	0.0519
	Mean	**0.718**	**0.215**	**0.222**	**0.709**	**0.0607**
	Standard error	0.014	0.028	0.016	0.030	0.0088
PP	1	0.551	0.161	0.165	0.673	0.0764
	2	0.578	0.169	0.178	0.692	0.0462
	3	0.657	0.210	0.269	0.870	0.0715
	Mean	**0.596**	**0.180**	**0.204**	**0.745**	**0.0647**
	Standard error	0.032	0.015	0.033	0.063	0.0094

For each run, the ODD values correspond to the mean across all the possible pairings of dark-adapted and bleached images. The coverage value was calculated from these mean values. The shape factor was obtained by fitting a negative Gaussian shape to the dark-adapted fluorescence levels once divided by the mean bleached fluorescence for the same illumination location.

conditions. The fluorescence returning through the photopigment layer provides a measure of the illumination intensity at the lipofuscin granules, which effectively serve as detectors in this case. That is, the logarithm of the ratio between intensities in Fig. 1 (a) and (b) provides a single pass estimate of the ODD of the photoreceptor layer. ODD_f changes with illumination position, with a maximum for illumination on the SC peak and decreasing values off peak.

In Fig. 2 we show a set of fluorescence images obtained for subject PP in a scan through the entry pupil locations. The shallow peak visible in each image cannot be produced by cone directionality since: (a) its position is perfectly correlated with the illumination position and (b) its height remains approximately constant, independent of the bleaching state of the photopigments and pupil position. We attribute this to lens fluorescence.

We further confirmed the lack of directionality of the fluorescence light by comparing the density difference maps (Fig. 3) for reflectometry and fluorescence. The estimates have been obtained from the pixel-to-pixel ratio between mean images for one of the experimental

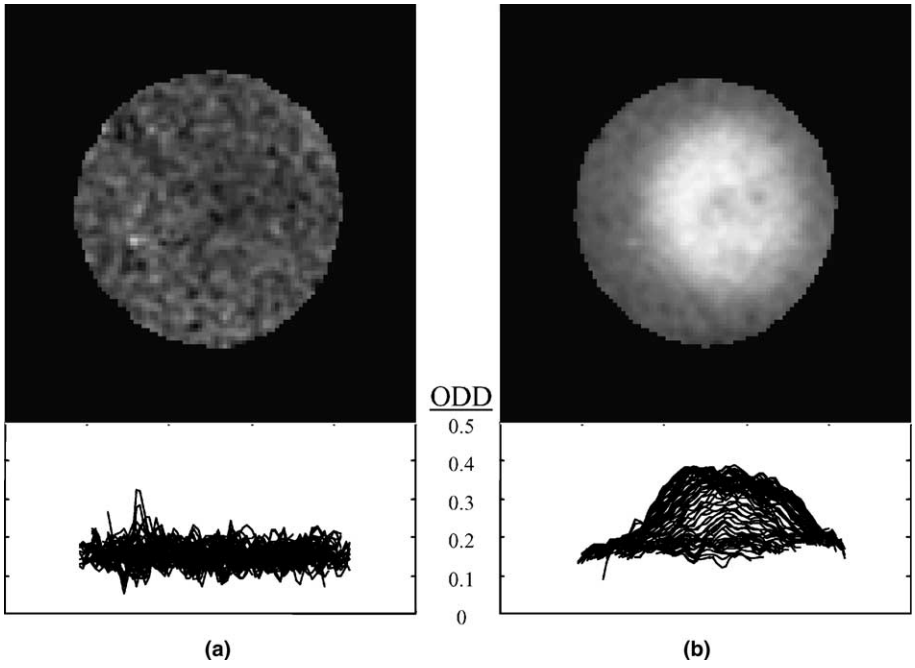

Fig. 3. Fluorescence (panel a) and reflectometry (panel b) optical density difference maps from the mean images calculated by averaging all the on-peak images for each experimental condition (dark-adapted fluorescence, bleached fluorescence, dark-adapted reflectometry and bleached reflectometry) obtained in one of the experimental runs in subject PP.

runs on subject PP. The reflectometry density difference map shows a clear peak (whose location coincides with the subject's OSC peak), whereas the fluorescence density difference map is noisy but essentially flat.

4. Discussion

4.1. Comparison of fluorescence and directional on-peak ODD estimates: estimating the cone coverage factor

The absence of a directional peak in the lipofuscin fluorescence condition suggests that the light originating in the RPE does not couple well with the photoreceptors and is not guided back towards the pupil. By analogy, it can be assumed that light scattered deeper in the RPE or choroid also does not couple well to the outer segments nor does it get guided back towards the pupil (see van de Kraats et al., 1996 for a discussion). Therefore, the directional peaks in the reflectometric images must arise from reflections internal to the cones. That is, some proportion of the light that has been guided on its way into the cones is reflected within the cone, and in turn guided back towards the pupil, traveling through the cones twice. The reflection is assumed by this model to occur either due to an impedance change at the base of the outer segment, or due to coupled scattering just distal to the outer segment (Gorrand & Delori, 1997). In that case, the directional optical density difference can be expressed as

$$\mathrm{ODD_d} = 2L\delta \tag{1}$$

where L stands for the length of a cone and δ is the photopigment optical density per unit length. While this equation assumes a complete double pass, other models (van de Kraats et al., 1996) propose that there are reflections between cone discs. If this were the case, $2L$ would represent the average path length of light within the outer segments.

In the fluorescence conditions, there is no double pass through the photoreceptors. In a first order model of light pathways, two sets of rays can be considered to excite the lipofuscin: guided rays escaping the photoreceptor, which we will assume to traverse a single photoreceptor length, L; and unguided rays, which we will consider to reach the RPE entirely through the interphotoreceptor matrix. The fraction of rays following the former pathway equals the ratio between the effective light-capturing area of the photoreceptor array and the total area of the retina, i.e., the optical coverage factor, C. If we compare the fluorescence level in dark-adapted conditions, F_{da}, with that obtained after bleaching, F_{bl}, a fraction $C \cdot F_{\mathrm{bl}}$ of the latter corresponds to guided rays and is attenuated by a factor $10^{-L\delta}$ in the presence of photopigments, while the fluorescence from unguided rays $(1 - C) \cdot F_{\mathrm{bl}}$, remains unaltered. Accordingly, these two fluorescence levels can be related as

$$F_{\mathrm{da}} = CF_{\mathrm{bl}}10^{-L\delta} + (1 - C)F_{\mathrm{bl}} \tag{2}$$

The ratio between them can be expressed as

$$\frac{F_{\mathrm{da}}}{F_{\mathrm{bl}}} = 10^{-\mathrm{ODD_f}} = 10^{-L\delta}C + (1 - C) \tag{3}$$

The negative logarithm of this value is the fluorescence optical density difference, $\mathrm{ODD_f}$.

By combining Eqs. (1) and (3), we can obtain an estimate of the coverage factor as a function of the directional reflection and fluorescence ODDs:

$$C = \frac{10^{-\mathrm{ODD_f}} - 1}{10^{-\frac{1}{2}\mathrm{ODD_d}} - 1} \tag{4}$$

In Table 1, the coverage factor estimates can be seen for three runs for each subject, obtained from the $\mathrm{ODD_d}$ and $\mathrm{ODD_f}$ mean values across all the possible pairings of dark-adapted and bleached images. Mean coverage values around 70–75% are obtained. Although these are estimates of optical rather than anatomical coverage, the values are compatible with histological data (Candy, Crowell, & Banks, 1998; Miller & Bernard, 1983). While a more complete model, taking into account leakage of light from the cones could improve the estimates, these effects appear to occur primarily for high angles of incidence (Chen & Makous, 1989), and are expected to produce only minor changes in the calculations. Finally, in our procedure we implicitly suppose the optical properties of the RPE to remain constant. Although there is a high level metabolic activity following photopigment bleaching, there is not evidence that there are significant changes occurring for our wavelengths over the time scale of these experiments. The slow changes reported by DeLint et al. (2000) may arise from changes at the RPE, but control experiments under our conditions were performed to rule out a contribution from these slow changes.

4.2. Comparison of fluorescence and background ODD estimates: intraocular scattering and anterior reflections

We have found that the background intensity is modulated by the amount of photopigment present. This requires that a fraction of the multiply scattered light travels in part through the photoreceptors outer segments. However, the lack of directionality in the fluorescence suggests that the light from deeper retinal layers does not couple well with the outer-most end of the photoreceptors. As a result it appears that the passage through the cone outer segments is on the first pass through the photoreceptor layer. Thus, for the background component of the reflected light, the density difference will be identical to the fluorescence density difference, minus a component that arises due to any

anterior reflectors (Delori & Pflibsen, 1989; van Norren & Tiemeijer, 1986), which return light to the pupil prior to passage through the photoreceptors. We find that the ODD_d, values for our subjects are not significantly different from ODD_b (see Table 1). This is most likely because our subjects were young and had clear optics, and any retinal scattering was in a forward direction. However, the situation could be quite different for subjects with more turbid ocular media. In that case, the amount of background light sensitive to the photopigments would be greatly reduced, and, as a consequence, the background ODD should be smaller than the fluorescence ODD. The difference between these two ODD estimates could, perhaps, be used to quantify the turbidity of the ocular media in such subjects. This quantification is likely to be feasible only for small amounts of intraocular scattering, since the fluorescence signal is too low to measure major reductions. However, since lipofuscin concentration increases with age (Delori, Goger, & Dorey, 2001), the measurement could become more reliable with increasing age, where scatter is of more clinical interest.

Additionally, there is conflicting evidence relating light exposure to changes in choroidal blood volume (see Longo, Geiser, & Riva, 2000), Such changes presumably arise from an active mechanism regulating the temperature of the outer retinal layers. However, due to the low absorption of hemoglobin in the spectral range of the lipofuscin measurements, the fluorescence measurements should be less affected by any changes in blood volume than the 543 nm diffuse reflection, and therefore, the background and fluorescence ODD estimates could be affected by different amounts. While spectral analysis of the fluorescence or measurement with a different illumination wavelength would allow us to analyze this potential problem, they are beyond the scope of this paper. However, the reported changes in the choroidal blood volume were around 10% and the potential effect of changes in blood absorption would be only a fraction of this since not all the involved pathways of the light traverse this blood. As a consequence, the maximal difference induced in the ODD estimates is expected to be considerably smaller than the precision of our method.

4.3. Single pass OSC peak width from fluorescence

Although there is excellent agreement between the pupil positions for cone directionality measured psychophysically and optically, the OSC peak is narrower than its psychophysical counterpart (DeLint et al., 1997; He et al., 1999). To further explore this result, we analyzed the dependence of the ODD_f on pupil entry position. For this analysis, we treated the amount of light reaching the RPE as approximately constant when the cone photopigments were bleached. This assumption is based on the low total reflectance of the retina. On the contrary, the intensity of light reaching the RPE when the photopigments are fully regenerated will be at its minimum when the illumination is on the SC peak and will increase off-peak since the absorption decreases as the coupling to the photoreceptors decreases. Assuming a Gaussian shape for the coupling efficiency, the dark-adapted fluorescence for an entry position separated a distance r from the SC peak is related to the bleached fluorescence for the same entry position as

$$F_{da}(r) = F_{bl}(r)(1 - A10^{-\rho r^2}) \quad (5)$$

where A represents the maximum attenuation due to photopigment absorption that occurs for on-peak illumination.

Ideally, the bleached fluorescence, F_{bl}, should be constant with the distance r. However, experimentally the intensity reaching the eye was found to change with the illumination location, especially in the vicinity of the system pupil. Accordingly, it is convenient to calculate the ratio between $F_{da}(r)$ and $F_{bl}(r)$ for each pupil position, r, which should correspond to a negative Gaussian shape

$$F_{da}(r)/F_{bl}(r) = (1 - A10^{-\rho r^2}) \quad (6)$$

To calculate this ratio, we divided the average intensity level in each dark-adapted image by the mean intensity across the bleached images for the same intended illumination position. The set of values was then fit to a negative Gaussian shape.

In Table 1 we have represented the Gaussian shape factor, ρ, obtained for each subject, with its standard deviation across runs. These values can be seen to be closer to the psychophysical SC ρ values, typically around 0.05 mm^{-2}, than to the reflectometry SC ρ values, around 0.1 mm^{-2} for an entry-scanning exit-non-scanning setup (He et al., 1999; van Blokland, 1986) and also slightly broader than the multiple entry measurements of the directed light return of Marcos and Burns (1999). This result supports the idea that the difference in shape between the optical and psychophysical SC peaks is due to the second pass through the photoreceptor layer. One possible contributing factor could be the coherent interaction between the guided reflections coming from photoreceptors with slightly different lengths, as proposed by Marcos and Burns (1999) and Marcos et al. (1998), together with a loss of light from waveguide modes which are partially guided through the outer segments.

5. Conclusions

We have demonstrated that lipofuscin fluorescence can be used as a tool for probing the single-pass optical density of the photoreceptor layer. The lack of direction-

ality of the fluorescence signal allows us to conclude that the directional component of the retinal reflection arises from light which is guided into and, following internal reflection, guided out of the cone outer segments. Light that has escaped the outer segments is not recoupled to them in reflection. The ratio between fluorescence levels measured under dark-adapted and bleached conditions was used to estimate the single-pass photopigment optical density difference. Comparison of the single-pass density difference with the double pass density difference obtained from the guided reflectometric component of retinal reflectometry images yielded retinal coverage estimates around 75%. Additionally, the optical density difference for the multiply scattered background light was calculated from the retinal reflectometry data and found to be essentially identical to the fluorescence single pass estimates. Finally, the fluorescence intensity values obtained by varying the pupil entry position of the input illumination were fitted to obtain an estimate of the single pass optical Stiles–Crawford peak width. These values were in the range of those typically obtained for psychophysical measurements of the Stiles–Crawford effect, suggesting that other phenomena in addition to the cone waveguide properties are involved in the optical Stiles–Crawford effect.

Acknowledgment

Supported by NIH EY04395, and Human Frontier Science Program Organization Long Term Fellowship LT0326/1999-B (P. M. Prieto).

References

Berendschot, T. T., DeLint, P. J., & van Norren, D. (2003). Fundus reflectance-historical and present ideas. *Progress in Retinal and Eye Research, 22*, 171–200.

Burns, S. A., Wu, S., Delori, F. C., & Elsner, A. E. (1995). Direct measurement of human cone photoreceptor alignment. *Journal of the Optical Society of America A, 12*, 2329–2338.

Burns, S. A., Wu, S., He, J. C., & Elsner, A. E. (1997). Variations in photoreceptor directionality across the central retina. *Journal of the Optical Society of America A, 14*, 2033–2040.

Candy, T. R., Crowell, J. A., & Banks, M. S. (1998). Optical, receptoral, and retinal constraints on foveal and peripheral vision in the human neonate. *Vision Research, 38*, 3857–3870.

Chen, B., & Makous, W. (1989). Light capture by human cones. *Journal of Physiology-London, 414*, 89–109.

DeLint, P. J., Berendschot, T. T. J. M., van de Kraats, J., & van Norren, D. (2000). Slow optical changes in human photoreceptors induced by light. *Investigative Ophthalmology and Visual Science, 41*, 282–289.

DeLint, P. J., Berendschot, T. T. J. M., & van Norren, D. (1997). Local photoreceptor alignment measured with a scanning laser ophthalmoscope. *Vision Research, 37*, 243–248.

Delori, F. C. (1994). Spectrophotometer for noninvasive measurement of intrinsic fluorescence and reflectance of the ocular fundus. *Applied Optics, 33*, 7439–7452.

Delori, F. C., Dorey, C. K., Staurenghi, G., Arend, O., Goger, D. G., & Weiter, J. J. (1995). In vivo fluorescence of the ocular fundus exhibits retinal pigment epithelium lipofuscin characteristics. *Investigative Ophthalmology and Visual Science, 36*, 718–729.

Delori, F. C., Goger, D. G, & Dorey, C. K. (2001). Age-related accumulation and spatial distribution of lipofuscin in RPE of normal subjects. *Investigative Ophthalmology and Visual Science, 42*, 1855–1866.

Delori, F. C., & Pflibsen, K. P. (1989). Spectral reflectance of the human ocular fundus. *Applied Optics, 28*, 1061–1077.

Elsner, A. E., Burns, S. A., Hughes, G. W., & Webb, R. H. (1992). Reflectometry with a scanning laser ophthalmoscope. *Applied Optics, 31*, 3697–3710.

Elsner, A. E., Burns, S. A., & Webb, R. H. (1993). Mapping cone photopigment optical density. *Journal of the Optical Society of America A, 10*, 52–58.

Gorrand, J. M., & Delori, F. (1995). A reflectometric technique for assessing photoreceptor alignment. *Vision Research, 35*, 999–1010.

Gorrand, J. M., & Delori, F. C. (1997). A model for assessment of cone directionality. *Journal of Modern Optics, 44*, 473–491.

He, J. H., Marcos, S., & Burns, S. A. (1999). Comparison of cone directionality determined by psychophysical and reflectometric techniques. *Journal of the Optical Society of America A, 16*, 2363–2369.

Kilbride, P. E., Read, J. S., Fishman, G. A., & Fishman, M. (1983). Determination of human cone pigment density difference spectra in spatially resolved regions of the fovea. *Vision Research, 23*, 1341–1350.

Longo, A., Geiser, M., & Riva, C. E. (2000). Subfoveal choroidal blood flow in response to light-dark exposure. *Investigative Ophthalmology and Visual Science, 41*, 2678–2683.

Marcos, S., & Burns, S. A. (1999). Cone spacing and waveguide properties from cone directionality measurements. *Journal of the Optical Society of America A, 16*, 995–1004.

Marcos, S., Burns, S. A., & He, J. C. (1998). Model for cone directional reflectometric measurements based on scattering. *Journal of the Optical Society of America A, 15*, 2012–2022.

Marcos, S., Tornow, R. P., Elsner, A. E., & Navarro, R. (1997). Foveal cone spacing and cone photopigment density difference: objective measurements in the same subjects. *Vision Research, 37*, 1909–1915.

Miller, W. H., & Bernard, G. D. (1983). Averaging over the foveal receptor aperture curtails aliasing. *Vision Research, 23*, 1365–1369.

Rushton, W. A. H. (1958). Kinetics of cone pigments measured objectively in the living human fovea. *Annals of the New York Academy of Science, 74*, 291–304.

Stiles, W. S., & Crawford, B. H. (1933). The luminous efficiency of rays entering the eye pupil at different points. *Proceedings of the Royal Society (London) B, 112*, 428–450.

Tornow, R. P., Beuel, S., & Zrenner, E. (1997). Modifying a Rodenstock scanning laser ophthalmoscope for imaging densitometry. *Applied Optics, 36*, 5621–5629.

van Blokland, G. J. (1986). Directionality and alignment of the foveal receptors, assessed with light scattered from the human fundus in vivo. *Vision Research, 26*, 495–500.

van de Kraats, J., Berendschot, T. T. J. M., & van Norren, D. (1996). The pathways of light measured in fundus reflectometry. *Vision Research, 36*, 2229–2247.

van Norren, D., & Tiemeijer, L. F. (1986). Spectral reflectance of the human eye. *Vision Research, 26*, 313–320.

van Norren, D., & van de Kraats, J. (1989). Imaging retinal densitometry with a confocal scanning laser ophthalmoscope. *Vision Research, 29*, 1825–1830.

Vohnsen, B., Iglesias, I., & Artal, P. (2004). Directional imaging of the retinal cone mosaic. *Optics Letters, 9*, 968–970.